

Double shadow of a 4D Einstein-Gauss-Bonnet black hole and their connection between with quasinormal modes

Tian-Tian Liu, He-Xu Zhang, Yu-Hang Feng, Jian-Bo Deng, and Xian-Ru Hu*

Institute of Theoretical Physics & Research Center of Gravitation,

Lanzhou University, Lanzhou 730000, China

Abstract

In this paper, we firstly study the shadow of a 4D Einstein-Gauss-Bonnet black hole as photons couple to the Weyl tensor and find that the propagation of light depends on its polarization which leads to the existence of a double shadow. Further, we discuss the effect of the coupling parameter λ , the polarization of light and the Gauss-Bonnet coupling constant α on shadow. Then we explore the influence of the Gauss-Bonnet coupling constant α on the quasinormal modes (QNMs) of massless scalar field and investigate the connection between the real part of QNMs in the eikonal limit and the modified shadow radius of black holes. We find that in the eikonal limit the real part of QNMs is inversely proportional to the shadow radius, which is also applicable in the case of the photons coupled to the Weyl tensor.

* Xian-Ru Hu: huxianru@lzu.edu.cn

I. INTRODUCTION

Einstein's general theory of relativity predicted the existence of black holes, which fascinate physicists over decades. Thus it is very important to detect black hole parameters for studying features of the black hole. Investigations show that observing the shadow of black hole provides a tentative way to obtain information as regards black hole [1–9]. In the last few years, the subject of black hole shadow aroused physicists' wide attention. As we all know, the shadow of black hole is determined by light rays that fall into an event horizon, which depends on the black hole parameters and the interaction between light and other fields. Drummond and Hathrell [10] first found that the superluminal photon propagation in gravitational backgrounds due to vacuum polarisation in QED induces interactions between the electromagnetic field and spacetime curvature. Then the coupled photons have been studied widely in refs.[11–18]. It indicates that the the interaction between electromagnetic field and curvature tensor changes the path of photons propagation and leads to the birefringence phenomenon of light.

On the other hand, the discovery of gravity waves has provided ue with a new window to understand the universe. It is well known that black hole perturbations result in the emission of gravitational (electromagnetic or scalar) waves, which are characterized by complex frequencies called quasinormal modes (QNMs). And QNMs have been investigated by using other analytic and numerical methods [19–26]. What's more, a connection between the shadow of black hole and QNMs has attracted a lot of attention in recent years. Cardoso *et al.* pointed out that in the eikonal limit, the real part of QNMs is connected to the last circular null geodesic in ref.[27], and Stefanov *et al.* found a connection between the black hole QNMs and the strong gravitation lensing in the strong field regime [28]. Then in recent works [29–33], Jusufi *et al.* explored the relationship between the shadow of black hole and

QNMs.

Our aim in this paper is to explore how the shadow of a 4D Einstein-Gauss-Bonnet black hole change as photons couple to the Weyl tensor and investigate the connection between the modified shadow radius and QNMs. It's worth noting that a general covariant GB modified gravity in four dimensions was proposed by rescaling the GB coupling parameter $\hat{\alpha} \rightarrow \frac{\alpha}{D-4}$ which completed the missing piece of the EGB gravity [34].

This paper is organized as follows. In Sec. II, we derive equations of motion for the photons coupled to the Weyl tensor in a 4D Einstein-Gauss-Bonnet black hole spacetime. Then we explore the change of the black hole shadow as photons couple to the Weyl tensor in Sec. III. In Sec. IV, we use the sixth-order WKB method to study the QNMs of scalar fields in a 4D Einstein-Gauss-Bonnet black hole spacetime. In Sec. V, we investigate the connection between the modified shadow radius and QNMs. Finally, we comment on our results in Sec. VI

II. EQUATION OF MOTION FOR THE PHOTONS COUPLED TO WEYL TENSOR

In this section, we begin with the action of the electromagnetic field coupled to Weyl tensor in the curved spacetime ,which can be expressed as [34, 35]

$$S = \int d^4 \sqrt{-g} \left[\frac{R}{16\pi G} + \frac{1}{16\pi G} \hat{\alpha} \mathcal{L}_{GB} - \frac{1}{4} (F_{\mu\nu} F^{\mu\nu} - 4\lambda C^{\mu\nu\rho\sigma} F_{\mu\nu} F_{\rho\sigma}) \right], \quad (1)$$

where $\hat{\alpha}$ is the the Gauss-Bonnet coupling with dimension of length-squared and $\mathcal{L}_{GB} = R_{\mu\nu}^{\rho\sigma} R_{\rho\sigma}^{\mu\nu} - 4R_{\mu}^{\nu} R_{\nu}^{\mu} + R^2$ is the Gauss-Bonnet invariant. $F_{\mu\nu} = \partial_{\mu} A_{\nu} - \partial_{\nu} A_{\mu}$ is the usual electromagnetic tensor. $C_{\mu\nu\rho\sigma}$ is the Weyl tensor, which is defined as $C_{\mu\nu\rho\sigma} = R_{\mu\nu\rho\sigma} - (g_{\mu[\rho} R_{\sigma]\nu} - g_{\nu[\rho} R_{\sigma]\mu}) + \frac{1}{3} R g_{\mu[\rho} g_{\sigma]\nu}$. And the photons coupled to the Weyl tensor can be characterized by the coupling parameter λ . Varying the action

(1) with respect to A_μ , we can obtain the corrected Maxwell equation

$$\nabla_\mu (F_{\mu\nu} - 4\lambda C_{\mu\nu\rho\sigma} F^{\rho\sigma}) = 0. \quad (2)$$

From the above corrected Maxwell equation (2), one can obtain the equation of motion of the coupled photons by the geometric optics approximation. Under this approximation, $\lambda_c < \lambda < L$, where λ is the wavelength of photon, L is a typical curvature scale, and λ_c is the electron compton wavelength [11–13, 36–39]. In this method, the electromagnetic field strength can be written as

$$F_{\mu\nu} = f_{\mu\nu} e^{i\theta}, \quad (3)$$

where $f_{\mu\nu}$ is a slowly varying amplitude and θ is a rapidly varying phase. The wave vector is defined as $k_\mu = \partial_\mu \theta$, which corresponds to the photon momentum in the quantum partial interpretation. According to the Bianchi identity, the amplitude $f_{\mu\nu}$ has the form $f_{\mu\nu} = k_\mu a_\nu - k_\nu a_\mu$, where a_μ can be interpreted as the polarization vector of photon and satisfies $k_\mu a^\mu = 0$. Inserting Eq.(3) into Eq.(2) and using the relationship above, we arrive at

$$k_\mu k^\mu a^\nu + 8\lambda C^{\mu\nu\rho\sigma} k_\sigma k_\mu a_\rho = 0. \quad (4)$$

Obviously, the coupling between Weyl tensor and electromagnetic field affects the propagation of the coupled photon in the background spacetime.

Let us now consider the 4D Einstein-Gauss-Bonnet black hole obtained by Glavan and Lin in [34], with the metric form

$$ds^2 = -f(r) dt^2 + f(r)^{-1} dr^2 + r^2(d\theta^2 + \sin^2\theta d\phi^2) \quad (5)$$

where

$$f(r) = 1 + \frac{r^2}{2\alpha} \left(1 \pm \sqrt{1 + \frac{8\alpha M}{r^3}} \right) \quad (6)$$

Here, the sign \pm refers to the two different branches, and we consider only the negative branch because that it gives a Schwarzschild-like solution in the asymptotically limit [34, 40–43].

Now introducing a local orthonormal frame. The appropriate basis 1-forms are e^a ($a = 0, 1, 2, 3$) with

$$e^0 = \sqrt{f}dt, \quad e^1 = \frac{1}{\sqrt{f}}dr, \quad e^2 = r d\theta, \quad e^3 = r \sin\theta d\phi. \quad (7)$$

Introducing the notation $U_{ab}^{01} = \delta_a^0 \delta_b^1 - \delta_a^1 \delta_b^0$ [10–13], etc., the Weyl tensor can be simplified as

$$C_{abcd} = \mathcal{A}(2U_{ab}^{01}U_{cd}^{01} - U_{ab}^{02}U_{cd}^{02} - U_{ab}^{03}U_{cd}^{03} + U_{ab}^{12}U_{cd}^{12} + U_{ab}^{13}U_{cd}^{13} - 2U_{ab}^{23}U_{cd}^{23}) \quad (8)$$

with

$$\mathcal{A} = -\frac{M(r^3 + 2M\alpha)\sqrt{1 + \frac{8M\alpha}{r^3}}}{(r^3 + 8M\alpha)^2} \quad (9)$$

To solve the equation of motion of photon, it is convenient to introduce the following linear combination of momentum components [10–13]

$$l_b = k^a U_{ab}^{01}, \quad m_b = k^a U_{ab}^{02}, \quad n_b = k^a U_{ab}^{03}, \quad (10)$$

together with the dependent combinations

$$p_b = k^a U_{ab}^{12}, \quad q_b = k^a U_{ab}^{13}, \quad r_b = k^a U_{ab}^{23}. \quad (11)$$

The equation of motion of the coupled photon (4) can be rewritten as a set of equations for the independent polarisation components $a \cdot l$, $a \cdot m$ and $a \cdot r$. Plugging Eq.(8) into Eq.(4), we therefore arrive at

$$\begin{pmatrix} K_{11} & 0 & 0 \\ K_{21} & K_{22} & K_{23} \\ 0 & 0 & K_{33} \end{pmatrix} \begin{pmatrix} a \cdot l \\ a \cdot m \\ a \cdot r \end{pmatrix} = 0 \quad (12)$$

with

$$\begin{aligned}
K_{11} &= (1 - 16\lambda\mathcal{A})(-k^0k^0 + k^1k^1) + (1 + 8\lambda\mathcal{A})(k^2k^2 + k^3k^3), \\
K_{21} &= -24\lambda\mathcal{A}k^1k^2, \\
K_{22} &= (1 + 8\lambda\mathcal{A})(-k^0k^0 + k^1k^1 + k^2k^2 + k^3k^3), \\
K_{23} &= 24\lambda\mathcal{A}k^0k^3, \\
K_{33} &= (1 + 8\lambda\mathcal{A})(-k^0k^0 + k^1k^1) + (1 - 16\lambda\mathcal{A})(k^2k^2 + k^3k^3).
\end{aligned} \tag{13}$$

The condition of Eq.(12) with the non-zero solution is $K_{11}K_{22}K_{33} = 0$. The first root $K_{11} = 0$ leads to the modified light cone

$$(1 - 16\lambda\mathcal{A})(-k^0k^0 + k^1k^1) + (1 + 8\lambda\mathcal{A})(k^2k^2 + k^3k^3) = 0, \tag{14}$$

which corresponds to the case of the polarisation vector a_μ is proportional to l_μ . The second root $K_{22} = 0$ corresponds to an unphysical polarisation and should be neglected. The third root is $K_{33} = 0$, i.e.,

$$(1 + 8\lambda\mathcal{A})(-k^0k^0 + k^1k^1) + (1 - 16\lambda\mathcal{A})(k^2k^2 + k^3k^3) = 0, \tag{15}$$

which means that the vector $a_\mu = \lambda r_\mu$.

The above discussion shows that the light cone condition depends not only on the coupling between the photon and the Weyl tensor, but also on the polarization of light. We know from Eqs.(14) and (15) that the velocities of the photons for the two polarizations are different, i.e., the phenomenon of gravitational birefringence. Moreover, the light cone conditions (14) and (15) imply that instead of following geodesic in the original metric, the coupled photons follow null geodesics of the effective metric $\gamma_{\mu\nu}$, i.e., $\gamma^{\mu\nu}k_\mu k_\nu = 0$ [44]. The effective metric for the coupled photon can be expressed as

$$ds^2 = -f(r) dt^2 + f(r)^{-1} dr^2 + r^2 W(r)^{-1} (d\theta^2 + \sin^2\theta d\phi^2) \tag{16}$$

The quantity $W(r)$ is

$$W(r) = \frac{r^6 \sqrt{1 + \frac{8M\alpha}{r^3}} + Mr^3(8\alpha\sqrt{1 + \frac{8M\alpha}{r^3}} - 8\lambda) - 16M^2\alpha\lambda}{r^6 \sqrt{1 + \frac{8M\alpha}{r^3}} + 32M^2\alpha\lambda + Mr^3(8\alpha\sqrt{1 + \frac{8M\alpha}{r^3}} + 16\lambda)}, \quad (17)$$

for photon with the polarization along $l_\mu(PPL)$ and is

$$W(r) = \frac{r^6 \sqrt{1 + \frac{8M\alpha}{r^3}} + 32M^2\alpha\lambda + Mr^3(8\alpha\sqrt{1 + \frac{8M\alpha}{r^3}} + 16\lambda)}{r^6 \sqrt{1 + \frac{8M\alpha}{r^3}} + Mr^3(8\alpha\sqrt{1 + \frac{8M\alpha}{r^3}} - 8\lambda) - 16M^2\alpha\lambda}, \quad (18)$$

for photon with the polarization along $r_\mu(PPR)$.

III. WEYL CORRECTIONS TO SHADOW RADIUS

In this subsection, we will discuss the shadow radius of black hole as photons couple to the Weyl tensor. In the effective metric (16), there exist two conserved quantities energy E and angular momentum L as follow

$$E = f(r)\dot{t}^2, \quad L = r^2 \sin^2\theta W(r)^{-1} \dot{\phi}, \quad (19)$$

where the dot over a symbol is the differentiation with respect to an affine parameter β . Using the condition $\gamma^{\mu\nu}k_\mu k_\nu = 0$ and $k_\mu = \frac{dx_\mu}{d\beta}$, one can obtain the equations of motion

$$\frac{r^4 \dot{r}^2}{W(r)^2} = R(r), \quad (20)$$

$$\frac{r^4 \dot{\theta}^2}{W(r)^2} = \Theta(\theta). \quad (21)$$

Here, $R(r)$ and $\Theta(\theta)$ are given by

$$R(r) = \frac{E^2 r^4}{W(r)^2} - \frac{(\mathcal{Q} + L^2)r^2 f(r)}{W(r)}, \quad (22)$$

$$\Theta(\theta) = \mathcal{Q} - L^2 \cot^2\theta, \quad (23)$$

with \mathcal{Q} denoting the Carter constant [45]. To determine the geometric sharp of the shadow of the effective metric, Using the unstable condition

$$R(r) = 0, \quad \frac{dR(r)}{dr} = 0, \quad \frac{d^2R(r)}{dr^2} > 0. \quad (24)$$

One can obtain that

$$2f(r)W(r) - rf'(r)W(r) - rf(r)W'(r) = 0. \quad (25)$$

By solving this equation, one can determine the radius of the photon sphere r_{ps} . In particular, combining Eq.(24) with celestial coordinates [46]

$$x = \lim_{r_0 \rightarrow \infty} (-r_0^2 \sin\theta \frac{d\phi}{dr}), \quad y = \lim_{r_0 \rightarrow \infty} (r_0^2 \frac{d\theta}{dr}). \quad (26)$$

Where taking the limit $r_0 \rightarrow \infty$ according to the location of the observer and assuming the observer is situated in the equatorial plane ($\theta_0 = \frac{\pi}{2}$), one can express the radius of the shadow R_{sh} of the effective metric by the simple relation

$$R_{sh} = \sqrt{x^2 + y^2} = \frac{r_{ps}}{\sqrt{W(r_{ps})f(r_{ps})}}. \quad (27)$$

Here, we set $M = 1$, the variation of R_{sh} with parameter λ of the photons couple to the Weyl tensor and the GB coupling constant α for PPL and PPR in Figs.1 and 2, respectively. It is worth noting that the metric function may not be real inside the event horizon when α is too negative [40–43].

From Fig.1, we find that the black hole shadow depends on the coupling parameter λ and the polarization of light for different values of α . With the increase of the coupling parameter λ , the shadow radius R_{sh} for different values of α increases for PPL and decreases for PPM. Moreover, with the increase of the GB coupling parameter α , the shadow radius R_{sh} decreases for different polarizations of photons in Fig.2. The shadow radius R_{sh} of PPL is different from that of PPR in Fig.2 for fixed value of λ , which means the birefringence phenomenon occurs exactly in this

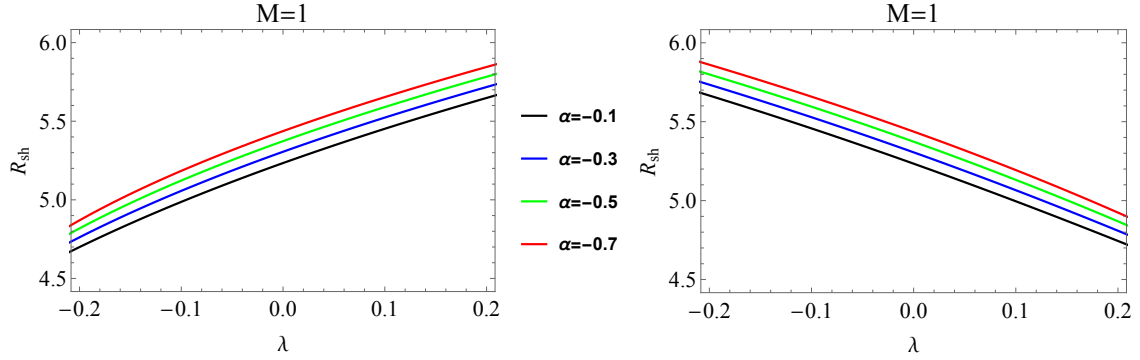


Figure 1: Variation of the shadow radius R_{sh} with the coupling parameter λ in a 4D Einstein-Gauss-Bonnet black hole spacetime. The left and the right are for PPL and PPR, respectively.

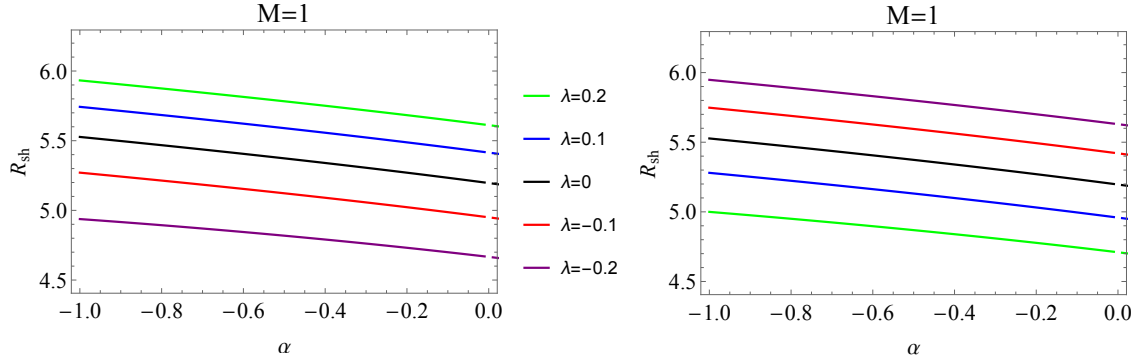


Figure 2: Variation of the shadow radius R_{sh} with the GB coupling parameter α in a 4D Einstein-Gauss-Bonnet black hole spacetime. The left and right are for PPL and PPR, respectively.

cause with non-vanishing λ . However, as $\lambda \rightarrow 0$, $W(r) \rightarrow 1$, one can find that the birefringence phenomenon vanish and the shadow radius can be reduced to that of usual photon.

IV. QNMS OF SCALAR FIELD

Considering a massless scalar field perturbation in the metric (5), it satisfies the Klein-Gorden equation

$$\frac{1}{\sqrt{-g}}\partial_\mu(\sqrt{-g}g^{\mu\nu}\partial_\nu\Phi) = 0. \quad (28)$$

Involving a separation of variables, the function Φ for the scalar field is given in terms of the spherical harmonics

$$\Phi(t, r, \theta, \phi) = \frac{1}{r}e^{-i\omega t}Y_l(r, \theta)\Psi(r), \quad (29)$$

in which $e^{-i\omega t}$ represents the time evolution of the field. Inserting Eq.(29) into Eq.(28) and introducing a "tortoise" coordinate $dr_* = \frac{dr}{f(r)}$, we can show that the field perturbation equation is given by the Schrödinger wave-like equation

$$\frac{d^2\Psi}{dr_*^2} + (\omega^2 - V_S(r))\Psi = 0. \quad (30)$$

Under the positive real part, QNMs, by definition, satisfy the following boundary condition,

$$\Psi(r_*) = C_\pm \exp(\pm i\omega r_*), \quad r \rightarrow \infty \quad (31)$$

where ω can be further written in terms of the real and imaginary parts, i.e., $\omega = \omega_R - i\omega_I$. The real and imaginary parts of QNMs represent the oscillation frequency and the decay rate, respectively. The effective potential $V_S(r)$ in Eq.(30) can be written as

$$V_S(r) = \left[1 + \frac{r^2}{2\alpha} \left(1 - \sqrt{1 + \frac{8\alpha M}{r^3}} \right) \right] \times \left[\frac{l(l+1)}{r^2} - \frac{2\alpha + r^3 \sqrt{1 + \frac{8\alpha M}{r^3}}}{\alpha r^3 \sqrt{1 + \frac{8\alpha M}{r^3}}} \right] \quad (32)$$

where l denotes the multipole number. One can deduce from Fig.3 that the height of the potential barrier governed by the effective potential increases with multipole

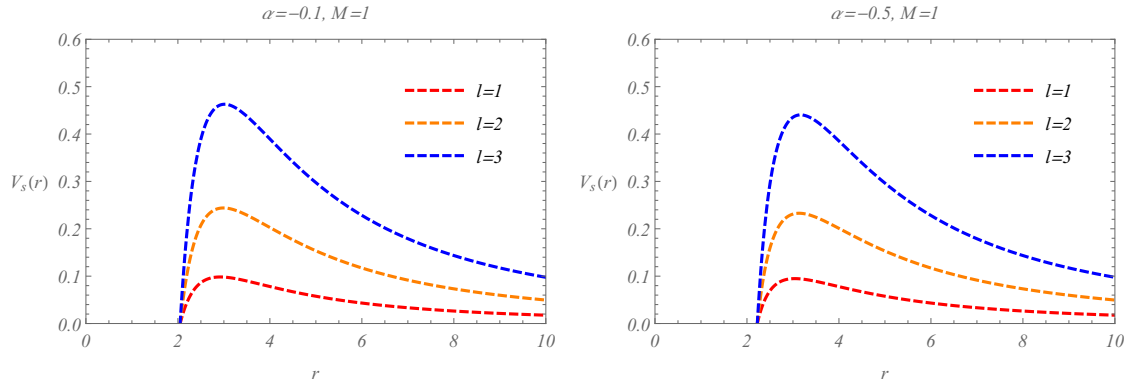


Figure 3: The figures are the effective potentials of the scalar field perturbation V_S for different values of the GB coupling constant α . Changing the parameter α changes the height of the potential barrier.

number l and the GB coupling parameter α . With the expression of the effective potential in hand, one can use the WKB approach to compute the QNMs frequencies. This method was proposed by Schutz and Will [19], then Iyer and Will extended the first WKB order formula to the third order [24]. In the present paper, we shall use the sixth-order WKB method which is described in [25] for calculating QNMs. We have presented the values of the QNMs for the scalar perturbation in Table I.

From Table I, we find that with the increase of the GB coupling parameter α , the real part of QNMs increases and the imaginary part decreases in absolute value. This particular effect can be clearly seen in Fig. 4. Moreover, we also see that higher absolute values of ω_I are obtained for the case $l = 2$ and $n = 1$, which means the scalar field perturbation damps more rapidly. It is worth noting that the WKB method works for $l > n$ (where n is the overtone number), otherwise, the accuracy is worse. So that we have not calculate the QNMs for the fundamental mode $l = 0, n = 0$, but can use the Frobenius method [47].

spin 0	l=1, n=0	l=2, n=0	l=2, n=1
α	$\omega(\text{WKB})$	$\omega(\text{WKB})$	$\omega(\text{WKB})$
-1	0.2593 - 0.1202i	0.4528 - 0.1097i	0.4203 - 0.3410i
-0.9	0.2643 - 0.1161i	0.4554 - 0.1085i	0.4241 - 0.3364i
-0.8	0.2688 - 0.1128i	0.4581 - 0.1073i	0.4281 - 0.3319i
-0.7	0.2728 - 0.1099i	0.4609 - 0.1060i	0.4322 - 0.3273i
-0.6	0.2765 - 0.1075i	0.4638 - 0.1048i	0.4365 - 0.3228i
-0.5	0.2798 - 0.1054i	0.4668 - 0.1035i	0.4409 - 0.3184i
-0.4	0.2828 - 0.1036i	0.4700 - 0.1023i	0.4453 - 0.3140i
-0.3	0.2855 - 0.1020i	0.4732 - 0.1010i	0.4499 - 0.3095i
-0.2	0.2881 - 0.1006i	0.4765 - 0.0996i	0.4544 - 0.3050i
-0.1	0.2905 - 0.0992i	0.4800 - 0.0982i	0.4591 - 0.3004i

Table I: The real and imaginary parts of quasinormal frequencies of the scalar field in the 4D Einstein-Gauss-Bonnet black hole spacetime with different coupling constant α .

V. CONNECTION BETWEEN THE SHADOW RADIUS AND QNMS

There is a main result was drawn by Cardoso *et al.* [27]. In the eikonal approximation, for any spherically symmetric spacetimes, the real part of the QNMs is given by the angular velocity of the unstable circular null geodesics while the imaginary part of the QNMs is related to the instability time scale of the orbit that can be represented by the Lyapunov exponent. What is more, Stefanov *et al.* published a paper in 2010 [28], which pointed out a connection between the black hole QNMs and the strong gravitation lensing in the strong field regime. In recent years, Jusufi found that in the eikonal limit the real part of QNMs is inversely proportional

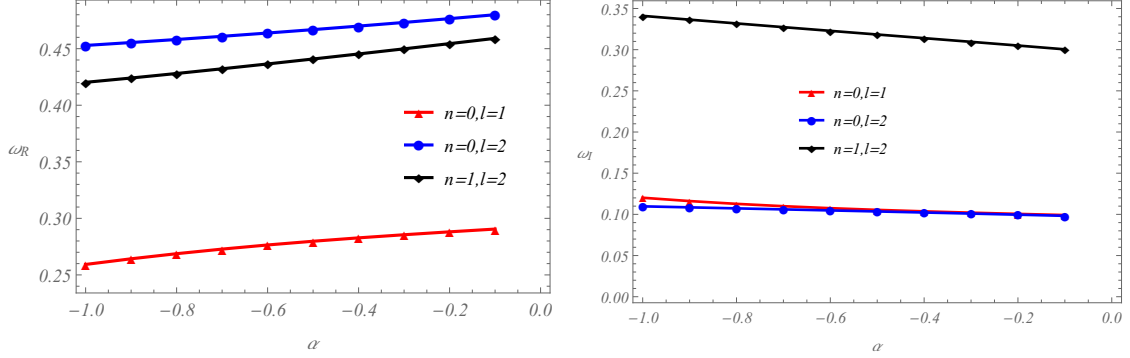


Figure 4: Left panel: Plots of the real part of the QNMs versus the GB coupling parameter α for the scalar field. Right panel: Plots of the imaginary part of QNMs versus the GB coupling parameter α . In both cases we have chosen $M = 1$.

to the shadow radius [29–31]

$$\omega_R \propto \frac{1}{R_{sh}}. \quad (33)$$

Further, the relationship between the real part of QNMs and the shadow radius can be expressed as

$$\omega_R = \lim_{l \gg 1} \frac{l}{R_{sh}}, \quad (34)$$

which is precise in the eikonal limit having large values of l . By this relationship, one obtains that the modified shadow radius decreases with the increase of the GB coupling constant α as the real part of QNMs increases. This effect is indeed shown to be the case in Fig. 2 and 4. We also list the results that the shadow radius R_{sh} with different GB coupling constant α in a 4D Einstein-Gauss-Bonnet black hole spacetime in Table II. Contrasting Table I with Table II, the relationship between the real part of QNMs and the modified shadow radius that satisfies Eq.(34) can be inferred approximately, even in the case of a small multipole number l . It can be

α	$R_{sh}(\text{PPL})$			$R_{sh}(\text{PPR})$		
	$\lambda = 0.1$	$\lambda = 0$	$\lambda = -0.1$	$\lambda = 0.1$	$\lambda = 0$	$\lambda = -0.1$
-1	5.7429	5.5270	5.2706	5.2801	5.5270	5.7478
-0.9	5.7138	5.4977	5.2426	5.2519	5.4977	5.7187
-0.8	5.6840	5.4678	5.2138	5.2230	5.4678	5.6890
-0.7	5.6535	5.4371	5.1843	5.1934	5.4371	5.6585
-0.6	5.6222	5.4056	5.1539	5.1629	5.4056	5.6273
-0.5	5.5901	5.3733	5.1226	5.1316	5.3733	5.5952
-0.4	5.5570	5.3400	5.0904	5.0992	5.3400	5.5623
-0.3	5.5231	5.3058	5.0571	5.0659	5.3058	5.5284
-0.2	5.4881	5.2705	5.0227	5.0314	5.2705	5.4934
-0.1	5.4519	5.2340	4.9871	4.9957	5.2340	5.4574

Table II: The shadow radius R_{sh} with different GB coupling constant α in a 4D Einstein-Gauss-Bonnet black hole spacetime.

interpreted as the decrease of the black hole horizon leads to the smaller shadow and the increase of oscillation frequencies.

VI. CONCLUSION

In this paper, we have studied the shadow of a 4D Einstein-Gauss-Bonnet black hole as the photon coupled to Weyl tensor and pointed out a simple connection between the modified shadow radius and the real part of QNMs. We found that the shadow of black hole depends not only on the GB coupling constant α , but also on the coupling parameter λ and the polarization of photon. For different polarizations of photon, the shadow radius R_{sh} decreases as the GB coupling constant

α increases. However, with a increase of the coupling parameter λ , the shadow radius R_{sh} increases for PPL and decreases for PPR.

Moreover, the connection between the modified shadow radius and the real part of QNMs satisfies Eq. (34) in the spacetime background of 4D Einstein-Gauss-Bonnet black hole. Computing the QNMs frequencies for the scalar field perturbation by the sixth-order WKB approach, we found that the real part of QNMs increases with the increase of the GB coupling constant α . Then using the correspondence between the geodesics and quasinormal spectrum, we pointed out the relationship between the shadow radius and the real part of QNMs, which is also applicable in the case of the photons coupled to the Weyl tensor. This may implies a potential connection between the shadow of black hole and gravitational wave. Recently, the result that the size of the shadow can reflect the phase structure of the axially symmetric black hole was explored in Ref. [48]. This suggests that QNMs in connection with the thermodynamic phase structure of the black hole and our work open a avenue for exploring this connection.

CONFLICTS OF INTEREST

The authors declare that there are no conflicts of interest regarding the publication of this paper.

ACKNOWLEDGMENTS

We would like to thank the National Natural Science Foundation of China (Grant No.11571342) for supporting us on this work. This work makes use of the Black Hole Perturbation Toolkit.

REFERENCES

- [1] JL Synge. The escape of photons from gravitationally intense stars. *Monthly Notices of the Royal Astronomical Society*, 131(3):463–466, 1966.
- [2] ID Novikov and KS Thorne. Black holes,(edited by c. dewitt and b. dewitt), 1973.
- [3] Subrahmanyan Chandrasekhar and Subrahmanyan Chandrasekhar. *The mathematical theory of black holes*, volume 69. Oxford university press, 1998.
- [4] Zdeněk Stuchlík, Daniel Charbulák, and Jan Schee. Light escape cones in local reference frames of kerr–de sitter black hole spacetimes and related black hole shadows. *The European Physical Journal C*, 78(3):1–32, 2018.
- [5] Arne Grenzebach, Volker Perlick, and Claus Lämmerzahl. Photon regions and shadows of accelerated black holes. *International Journal of Modern Physics D*, 24(09):1542024, 2015.
- [6] Farruh Atamurotov, Ahmadjon Abdujabbarov, and Bobomurat Ahmedov. Shadow of rotating non-kerr black hole. *Physical Review D*, 88(6):064004, 2013.
- [7] Sunny Vagnozzi and Luca Visinelli. Hunting for extra dimensions in the shadow of m87. *Physical Review D*, 100(2):024020, 2019.
- [8] Tian-Chi Ma, He-Xu Zhang, Peng-Zhang He, Hao-Ran Zhang, Yuan Chen, and Jian-Bo Deng. Shadow cast by a rotating and nonlinear magnetic-charged black hole in perfect fluid dark matter. *Modern Physics Letters A*, page 2150112, 2021.
- [9] Samuel E Gralla, Daniel E Holz, and Robert M Wald. Black hole shadows, photon rings, and lensing rings. *Physical Review D*, 100(2):024018, 2019.
- [10] Ian T Drummond and SJ Hathrell. Qed vacuum polarization in a background gravitational field and its effect on the velocity of photons. *Physical Review D*, 22(2):343,

1980.

- [11] RD Daniels and Graham M Shore. “faster than light” photons and charged black holes. *Nuclear Physics B*, 425(3):634–650, 1994.
- [12] RD Daniels and Graham M Shore. “faster than light” photons and rotating black holes. *Physics Letters B*, 367(1-4):75–83, 1996.
- [13] Rong-Gen Cai. Propagation of vacuum polarized photons in topological black hole spacetimes. *Nuclear Physics B*, 524(3):639–657, 1998.
- [14] Songbai Chen and Jiliang Jing. Strong gravitational lensing for the photons coupled to weyl tensor in a schwarzschild black hole spacetime. *Journal of Cosmology and Astroparticle Physics*, 2015(10):002, 2015.
- [15] He-Xu Zhang, Cong Li, Peng-Zhang He, Qi-Qi Fan, and Jian-Bo Deng. Optical properties of a brane-world black hole as photons couple to the weyl tensor. *The European Physical Journal C*, 80:1–11, 2020.
- [16] Songbai Chen, Shangyun Wang, Yang Huang, Jiliang Jing, and Shiliang Wang. Strong gravitational lensing for the photons coupled to a weyl tensor in a kerr black hole spacetime. *Physical Review D*, 95(10):104017, 2017.
- [17] Yang Huang, Songbai Chen, and Jiliang Jing. Double shadow of a regular phantom black hole as photons couple to the weyl tensor. *The European Physical Journal C*, 76(11):1–7, 2016.
- [18] Songbai Chen, Mingzhi Wang, and Jiliang Jing. Polarization effects in kerr black hole shadow due to the coupling between photon and bumblebee field. *Journal of High Energy Physics*, 2020(7):1–17, 2020.
- [19] Bernard F Schutz and Clifford M Will. Black hole normal modes: a semianalytic approach. *The Astrophysical Journal*, 291:L33–L36, 1985.
- [20] Valeria Ferrari and Bahram Mashhoon. New approach to the quasinormal modes of a black hole. *Physical Review D*, 30(2):295, 1984.

- [21] Subrahmanyan Chandrasekhar and Steven Detweiler. The quasi-normal modes of the schwarzschild black hole. *Proceedings of the Royal Society of London. A. Mathematical and Physical Sciences*, 344(1639):441–452, 1975.
- [22] Edward W Leaver. An analytic representation for the quasi-normal modes of kerr black holes. *Proceedings of the Royal Society of London. A. Mathematical and Physical Sciences*, 402(1823):285–298, 1985.
- [23] Gary T Horowitz and Veronika E Hubeny. Quasinormal modes of ads black holes and the approach to thermal equilibrium. *Physical Review D*, 62(2):024027, 2000.
- [24] Sai Iyer and Clifford M Will. Black-hole normal modes: A wkb approach. i. foundations and application of a higher-order wkb analysis of potential-barrier scattering. *Physical Review D*, 35(12):3621, 1987.
- [25] RA Konoplya. Quasinormal behavior of the d-dimensional schwarzschild black hole and the higher order wkb approach. *Physical Review D*, 68(2):024018, 2003.
- [26] Emanuele Berti, Vitor Cardoso, and Andrei O Starinets. Quasinormal modes of black holes and black branes. *Classical and Quantum Gravity*, 26(16):163001, 2009.
- [27] Vitor Cardoso, Alex S Miranda, Emanuele Berti, Helvi Witek, and Vilson T Zanchin. Geodesic stability, lyapunov exponents, and quasinormal modes. *Physical Review D*, 79(6):064016, 2009.
- [28] Ivan Zh Stefanov, Stoytcho S Yazadjiev, and Galin G Gylchev. Connection between black-hole quasinormal modes and lensing in the strong deflection limit. *Physical review letters*, 104(25):251103, 2010.
- [29] Kimet Jusufi. Quasinormal modes of black holes surrounded by dark matter and their connection with the shadow radius. *Physical Review D*, 101(8):084055, 2020.
- [30] Kimet Jusufi. Connection between the shadow radius and quasinormal modes in rotating spacetimes. *Physical Review D*, 101(12):124063, 2020.

- [31] Kimet Jusufi, Muhammed Amir, Md Sabir Ali, and Sunil D Maharaj. Quasinormal modes, shadow, and greybody factors of 5d electrically charged bardeen black holes. *Physical Review D*, 102(6):064020, 2020.
- [32] Cheng Liu, Tao Zhu, Qiang Wu, Kimet Jusufi, Mubasher Jamil, Mustapha Azreg-Ainou, and Anzhong Wang. Shadow and quasinormal modes of a rotating loop quantum black hole. *Physical Review D*, 101(8):084001, 2020.
- [33] M Ghasemi-Nodehi, Mustapha Azreg-Ainou, Kimet Jusufi, and Mubasher Jamil. Shadow, quasinormal modes, and quasiperiodic oscillations of rotating kaluza-klein black holes. *Physical Review D*, 102(10):104032, 2020.
- [34] Dražen Glavan and Chunshan Lin. Einstein-gauss-bonnet gravity in four-dimensional spacetime. *Physical review letters*, 124(8):081301, 2020.
- [35] Adam Ritz and John Ward. Weyl corrections to holographic conductivity. *Physical Review D*, 79(6):066003, 2009.
- [36] Graham M Shore. Faster than light photons in gravitational fields ii.: Dispersion and vacuum polarisation. *Nuclear Physics B*, 633(1-2):271–294, 2002.
- [37] Hing Tong Cho. “faster than light” photons in dilaton black hole spacetimes. *Physical Review D*, 56(10):6416, 1997.
- [38] VA De Lorenci, Renato Klippert, M Novello, and JM Salim. Light propagation in non-linear electrodynamics. *Physics Letters B*, 482(1-3):134–140, 2000.
- [39] Diego AR Dalvit, Francisco D Mazzitelli, and Carmen Molina-Paris. One-loop graviton corrections to maxwell’s equations. *Physical Review D*, 63(8):084023, 2001.
- [40] Timothy Clifton, Pedro Carrilho, Pedro GS Fernandes, and David J Mulryne. Observational constraints on the regularized 4d einstein-gauss-bonnet theory of gravity. *Physical Review D*, 102(8):084005, 2020.
- [41] Minyong Guo and Peng-Cheng Li. Innermost stable circular orbit and shadow of the 4 d einstein–gauss–bonnet black hole. *The European Physical Journal C*, 80(6):1–8,

2020.

- [42] RA Konoplya and AF Zinhailo. Quasinormal modes, stability and shadows of a black hole in the 4d einstein–gauss–bonnet gravity. *The European Physical Journal C*, 80(11):1–13, 2020.
- [43] Cheng-Yong Zhang, Peng-Cheng Li, and Minyong Guo. Greybody factor and power spectra of the hawking radiation in the 4 d einstein–gauss–bonnet de-sitter gravity. *The European Physical Journal C*, 80(9):1–9, 2020.
- [44] Oliver Preuss, Mark P Haugan, Sami K Solanki, and Stefan Jordan. An astronomical search for evidence of new physics: Limits on gravity-induced birefringence from the magnetic white dwarf re j0317-853. *Physical Review D*, 70(6):067101, 2004.
- [45] Brandon Carter. Global structure of the kerr family of gravitational fields. *Physical Review*, 174(5):1559, 1968.
- [46] Samuel E Vazquez and Ernesto P Esteban. Strong field gravitational lensing by a kerr black hole. *arXiv preprint gr-qc/0308023*, 2003.
- [47] RA Konoplya, Zdeněk Stuchlík, and A Zhidenko. Massive nonminimally coupled scalar field in reissner-nordström spacetime: Long-lived quasinormal modes and instability. *Physical Review D*, 98(10):104033, 2018.
- [48] Ming Zhang and Minyong Guo. Can shadows reflect phase structures of black holes? *The European Physical Journal C*, 80(8):1–9, 2020.